

## ORIGINAL ARTICLE

# CD40 is expressed in the subsets of endothelial cells undergoing partial endothelial–mesenchymal transition in tumor microenvironment

Kazuki Takahashi<sup>1,2</sup> | Miho Kobayashi<sup>1</sup>  | Hisae Katsumata<sup>1</sup> | Shiori Tokizaki<sup>1,3</sup> |  
 Tatsuhiko Anzai<sup>4</sup> | Yukinori Ikeda<sup>2</sup> | Daniel M. Alcaide<sup>2</sup> | Kentaro Maeda<sup>5</sup> |  
 Makoto Ishihara<sup>6</sup> | Katsutoshi Tahara<sup>7</sup> | Yoshiaki Kubota<sup>8</sup> | Fumiko Itoh<sup>9</sup>  |  
 Jihwan Park<sup>10</sup> | Kunihiko Takahashi<sup>4</sup> | Yukiko T. Matsunaga<sup>2</sup> | Yasuhiro Yoshimatsu<sup>1,5,11</sup> |  
 Katarzyna A. Podyma-Inoue<sup>1</sup>  | Tetsuro Watabe<sup>1,5</sup> 

<sup>1</sup>Department of Biochemistry, Graduate School of Medical and Dental Sciences, Tokyo Medical and Dental University, Tokyo, Japan

<sup>2</sup>Institute of Industrial Science, The University of Tokyo, Tokyo, Japan

<sup>3</sup>Department of Oral and Maxillofacial Surgical Oncology, Graduate School of Medical and Dental Sciences, Tokyo Medical and Dental University, Tokyo, Japan

<sup>4</sup>Department of Biostatistics, M&D Data Science Center, Tokyo Medical and Dental University, Tokyo, Japan

<sup>5</sup>Laboratory of Oncology, School of Life Sciences, Tokyo University of Pharmacy and Life Sciences, Tokyo, Japan

<sup>6</sup>Scientific Affairs Section, Life Science Sales Department, Life Science Business Division, Medical Business Group, Sony Corporation, Kanagawa, Japan

<sup>7</sup>Section 1, Product Design Department 2, Medical Product Design Division, Medical Business Group, Sony Corporation, Kanagawa, Japan

<sup>8</sup>Department of Anatomy, Keio University School of Medicine, Tokyo, Japan

<sup>9</sup>Laboratory of Stem Cells Regulations, Tokyo University of Pharmacy and Life Sciences, Tokyo, Japan

<sup>10</sup>School of Life Sciences, Gwangju Institute of Science and Technology (GIST), Gwangju, South Korea

<sup>11</sup>Division of Pharmacology, Graduate School of Medical and Dental Sciences, Niigata University, Niigata, Japan

## Correspondence

Tetsuro Watabe, Department of Biochemistry, Graduate School of Medical and Dental Sciences, Tokyo Medical and Dental University (TMDU), 1-5-45 Yushima, Bunkyo-ku, Tokyo 113-8549, Japan.  
 Email: [t-watabe.bch@tmd.ac.jp](mailto:t-watabe.bch@tmd.ac.jp)

## Funding information

Cooperation Program between TMDU, Sony Corporation and Sony Group Corporation; Japan Agency for Medical Research and Development, Grant/Award Number: JP21cm0106253 and

## Abstract

Tumor progression and metastasis are regulated by endothelial cells undergoing endothelial–mesenchymal transition (EndoMT), a cellular differentiation process in which endothelial cells lose their properties and differentiate into mesenchymal cells. The cells undergoing EndoMT differentiate through a spectrum of intermediate phases, suggesting that some cells remain in a partial EndoMT state and exhibit an endothelial/mesenchymal phenotype. However, detailed analysis of partial EndoMT has been hampered by the lack of specific markers. Transforming growth factor- $\beta$  (TGF- $\beta$ ) plays a central role in the induction of EndoMT. Here, we showed that inhibition of TGF- $\beta$  signaling

**Abbreviations:** CAF, cancer-associated fibroblast; CD40L, CD40 ligand; EMRECs, endothelial-mesenchymal transition reporter cells; EMT, epithelial-mesenchymal transition; EMT-TF, EMT transcription factor; EndoMT, endothelial-mesenchymal transition; GO, gene ontology; GSEA, gene set enrichment analysis; NES, normalized enrichment score; NG2, neural/glia antigen 2; OSCC, oral squamous cell carcinoma; PAI-1, plasminogen activator inhibitor-1; PECAM-1, platelet and endothelial cell adhesion molecule-1; qRT-PCR, quantitative RT-PCR; scRNA-seq, single-cell RNA sequencing; SM22 $\alpha$ , smooth muscle protein 22 $\alpha$ ; TGF- $\beta$ , transforming growth factor- $\beta$ ; Tie2, tunica interna endothelial cell kinase 2; TME, tumor microenvironment; TNF- $\alpha$ , tumor necrosis factor- $\alpha$ ; T $\beta$ RI, transforming growth factor- $\beta$  type I receptor; T $\beta$ RII, transforming growth factor- $\beta$  type II receptor; VE-cadherin, vascular endothelial cadherin; VEGFR2, vascular endothelial growth factor receptor 2;  $\alpha$ SMA,  $\alpha$ -smooth muscle actin.

Kazuki Takahashi and Miho Kobayashi contributed equally to this work.

This is an open access article under the terms of the [Creative Commons Attribution-NonCommercial-NoDerivs](https://creativecommons.org/licenses/by-nc-nd/4.0/) License, which permits use and distribution in any medium, provided the original work is properly cited, the use is non-commercial and no modifications or adaptations are made.  
 © 2023 The Authors. *Cancer Science* published by John Wiley & Sons Australia, Ltd on behalf of Japanese Cancer Association.

JP22ama221205; Japan Science and Technology Corporation, Grant/Award Number: JPMJSP2120; Japan Society for the Promotion of Science, Grant/Award Number: JP15K21394, JP19K07674, JP20H03851, JP20J11926, JP20K10111 and JP21J01294; Nanken-Kyoten, TMDU

suppressed EndoMT in a human oral cancer cell xenograft mouse model. By using genetic labeling of endothelial cell lineage, we also established a novel EndoMT reporter cell system, the EndoMT reporter endothelial cells (EMRECs), which allow visualization of sequential changes during TGF- $\beta$ -induced EndoMT. Using EMRECs, we characterized the gene profiles of multiple EndoMT stages and identified CD40 as a novel partial EndoMT-specific marker. CD40 expression was upregulated in the cells undergoing partial EndoMT, but decreased in the full EndoMT cells. Furthermore, single-cell RNA sequencing analysis of human tumors revealed that CD40 expression was enriched in the population of cells expressing both endothelial and mesenchymal cell markers. Moreover, decreased expression of CD40 in EMRECs enhanced TGF- $\beta$ -induced EndoMT, suggesting that CD40 expressed during partial EndoMT inhibits transition to full EndoMT. The present findings provide a better understanding of the mechanisms underlying TGF- $\beta$ -induced EndoMT and will facilitate the development of novel therapeutic strategies targeting EndoMT-driven cancer progression and metastasis.

#### KEYWORDS

CD40, EMT (epithelial–mesenchymal transition), EndMT (endothelial–mesenchymal transition), EndoMT (endothelial–mesenchymal transition), TGF- $\beta$

## 1 | INTRODUCTION

The tumor microenvironment (TME) comprises cancer cells, endothelial cells, cancer-associated fibroblasts (CAFs), immune cells, and other stroma cells.<sup>1</sup> Interactions between these components of the TME, through direct cell–cell contact or secretion of various cytokines and growth factors, promote tumor progression and metastasis.<sup>1,2</sup> Multiple lines of evidence suggest that transforming growth factor- $\beta$  (TGF- $\beta$ ) plays important roles in regulating TME networks.<sup>3</sup> TGF- $\beta$  binds to serine–threonine kinase type receptors (TGF- $\beta$  type I and type II receptors; T $\beta$ RI and T $\beta$ RII)<sup>4</sup> and phosphorylates Smad2/3. Phosphorylated Smad2/3 form a complex with Smad4, translocate into the nucleus, and regulate the transcription of various target genes, including plasminogen activator inhibitor-1 (PAI-1).

TGF- $\beta$  contributes to tumor progression and metastasis by inducing epithelial–mesenchymal transition (EMT) in epithelial cancer cells, leading to cancer cell invasion and metastasis.<sup>3,5–7</sup> EMT also confers cancer cells with resistance to chemotherapy and radiotherapy. In addition, TGF- $\beta$  induces tumor angiogenesis, immune tolerance, and the formation of CAFs. Thus, TGF- $\beta$  regulates tumor progression and metastasis by affecting various components of TME.

TGF- $\beta$  also induces endothelial–mesenchymal transition (EndoMT; also termed EndMT), which plays a role in tumor progression and metastasis.<sup>8,9</sup> During EndoMT, endothelial cells lose their characteristics such as strong cell–cell contact and the expression of endothelial cell-specific markers, including vascular endothelial growth factor receptor 2 (VEGFR2) and tunica interna endothelial cell kinase 2 (Tie2), and acquire mesenchymal phenotypes such as high motility and the expression of mesenchymal cell markers, including smooth muscle protein 22 $\alpha$  (SM22 $\alpha$ ) and  $\alpha$ -smooth muscle actin ( $\alpha$ SMA). We have previously reported that tumor necrosis

factor- $\alpha$  (TNF- $\alpha$ ) enhances TGF- $\beta$ -induced EndoMT to generate TGF- $\beta$ 2-secreting CAF-like cells that induce EMT in oral squamous cell carcinoma (OSCC) cells.<sup>10</sup> During cancer metastasis to distant organs, vascular integrity is reduced to facilitate cancer cell intravasation and extravasation. We have previously reported that extracellular vesicles released by TGF- $\beta$ -stimulated OSCC cells decrease the barrier function of endothelial cells accompanying induction of EndoMT.<sup>11</sup> Recent lines of evidence have also shown that EndoMT plays a role in tumor angiogenesis.<sup>12,13</sup> Although EndoMT has been implicated in various steps of cancer progression and metastasis, the molecular mechanisms underlying EndoMT remain to be elucidated.

Previous studies focusing on developmental EndoMT considered the transition of endothelial cells into mesenchymal cells as a permanent shift between two differentiated cell types; however, recent reports suggest a high plasticity of EndoMT.<sup>9</sup> It is now widely recognized that cells undergoing EndoMT differentiate through a spectrum of intermediary phases. This plasticity implies that some endothelial cells retain endothelial/mesenchymal hybrid characteristics and remain in a partial EndoMT state. Notably, this partial EndoMT state can be reversed under certain conditions.<sup>9</sup> Partial EndoMT has also been observed during angiogenesis.<sup>14,15</sup> However, the lack of experimental systems and specific markers for the identification of cells in partial EndoMT has hampered the detailed analysis of their characteristics.

To characterize the EndoMT-driven mesenchymal cells, several transgenic mouse models have been developed using endothelial lineage tracing to genetically label vascular endothelial cells.<sup>16,17</sup> Although such endothelial lineage tracing is useful for the analysis of EndoMT, the stepwise transition of EndoMT has not been identified yet.

In the present study, we established EndoMT reporter endothelial cells (EMRECs), a novel EndoMT reporter system, that enables the

visualization of sequential changes during EndoMT. Using EMRECs, we characterized the gene profiles of multiple EndoMT stages and succeeded in the identification of a novel partial EndoMT-specific marker. We also showed that cells representing a partial EndoMT state could be detected in the human tumors using single-cell RNA sequencing (scRNA-seq) analysis.

## 2 | MATERIALS AND METHODS

### 2.1 | Cell culture and reagents

Mouse EMRECs were established as described in “Supporting Information” and maintained in RPMI 1640 medium (Nacalai Tesque, Kyoto, Japan) containing 10% FBS (Thermo Fisher Scientific, Waltham, MA, USA), 100 units/mL penicillin, and 100  $\mu$ g/mL streptomycin (Nacalai Tesque). MS1, mouse endothelial cell line, was purchased from the ATCC (Manassas, VA, USA) and maintained in  $\alpha$ -Minimal Essential Medium ( $\alpha$ MEM; FUJIFILM Wako Pure Chemical, Osaka, Japan) supplemented with 10% FBS, 100 units/mL penicillin, and 100  $\mu$ g/mL streptomycin. SAS, human OSCC cell line, was obtained from RIKEN Bioresource Center Cell Bank (Tsukuba, Japan) and maintained in DMEM (Nacalai Tesque) supplemented with 10% FBS, 100 units/mL penicillin, and 100  $\mu$ g/mL streptomycin. TGF- $\beta$ 2 was purchased from Peprotech (Rocky Hill, NJ, USA).

### 2.2 | RNA isolation and quantitative RT-PCR

Total RNAs from MS1 cells or EMRECs were isolated using Sepasol I-RNA I Super G (Nacalai Tesque), the RNeasy Plus Mini kit (QIAGEN, Hilden, Germany), or the RNeasy FPE Kit (QIAGEN) and reversely transcribed using the PrimeScript II 1st strand cDNA Synthesis Kit (TaKaRa Bio, Otsu, Japan), the PrimeScript IV 1st strand cDNA Synthesis Kit (TaKaRa Bio), or ReverTraAce qPCR RT Mix (TOYOBO, Osaka, Japan). The quantitative RT-PCR (qRT-PCR) was performed with the Step One Plus Real-Time PCR System (Applied Biosystems, Waltham, MA, USA) or QuantStudio 3 (Applied Biosystems) using gene-specific primers and Fast Start Universal SYBR Green Master (Roche, Basel, Switzerland) or PowerUp SYBR Green Master Mix (Applied Biosystems). All expression data were normalized to the expression of  $\beta$ -actin. The primers used for qRT-PCR are listed in Table S1.

### 2.3 | Preparation of a three-dimensional microvessel on a chip

The  $25 \times 25 \times 5$  mm<sup>3</sup> polydimethylsiloxane (PDMS)-based chips were prepared as previously described.<sup>18,19</sup> To prepare three-dimensional (3D) microvessels, the PDMS chips were treated with O<sup>2</sup> plasma, sterilized with ultraviolet light and filled with ice-cold neutralized collagen solution comprising 3 mg/mL collagen type I (Cellmatrix Type I-A; pH3.0; Nitta Gelatin, Osaka, Japan), 10 $\times$  Hank's buffer

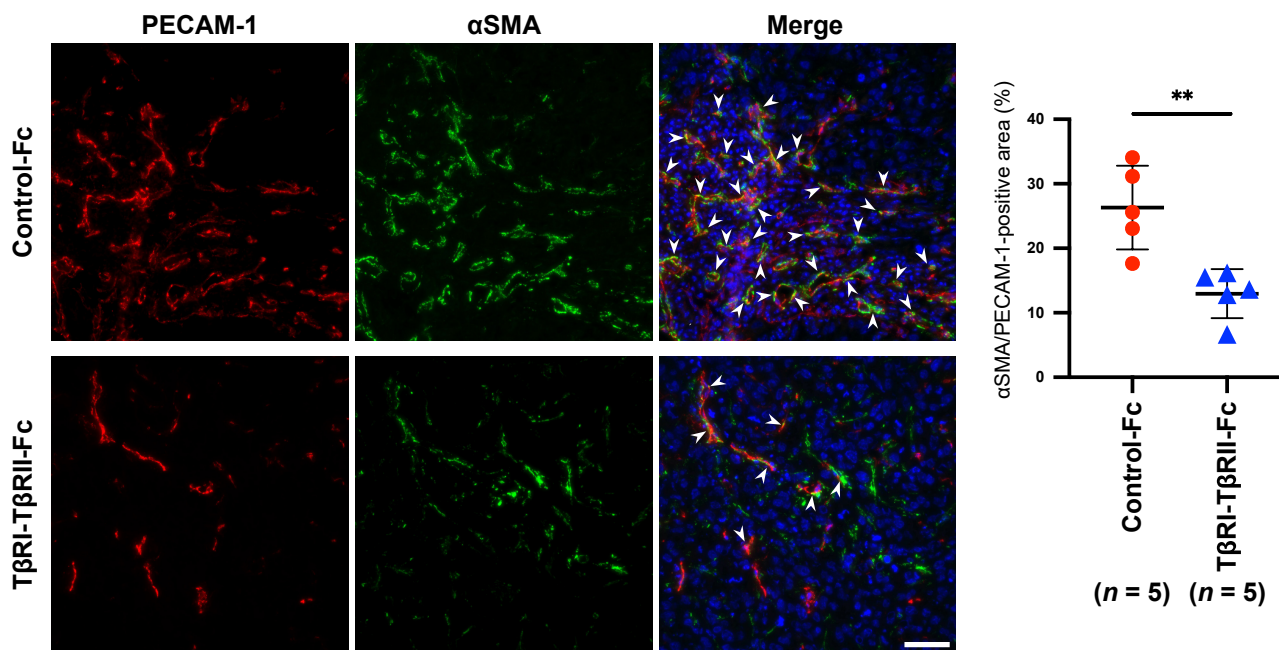


**FIGURE 1** Administration of recombinant T $\beta$ RI-T $\beta$ RII-Fc protein suppresses the formation of cells co-expressing endothelial and mesenchymal cell markers in primary tumors. Primary tumors from the mice administered with Control-Fc or T $\beta$ RI-T $\beta$ RII-Fc proteins were excised at day 76 post-injection and subjected to immunohistochemistry to examine the expression of endothelial cell marker, PECAM-1, and mesenchymal cell marker,  $\alpha$ SMA. Representative immunohistochemical images of staining for PECAM-1 (red),  $\alpha$ SMA (green), and nuclei (blue) and quantitative analysis. Arrowhead indicates  $\alpha$ SMA-positive area overlapping with PECAM-1-positive area. Values represent the ratio (%) of the  $\alpha$ SMA/PECAM-1-positive area in each primary tumor.  $n = 5$ . All data are represented as mean  $\pm$  SD. Scale bar: 50  $\mu$ m. Statistical analyses: two-tailed unpaired Student's  $t$ -test; \*\* $p < 0.01$ .

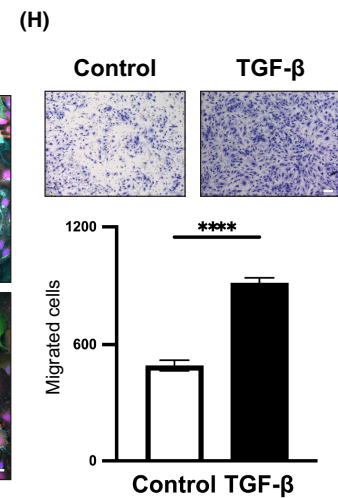
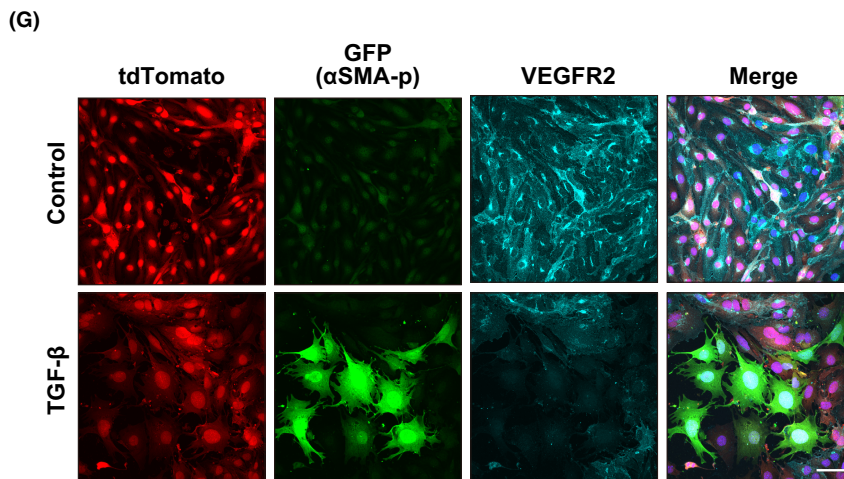
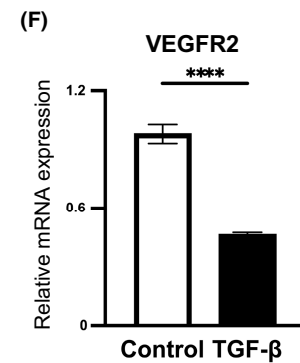
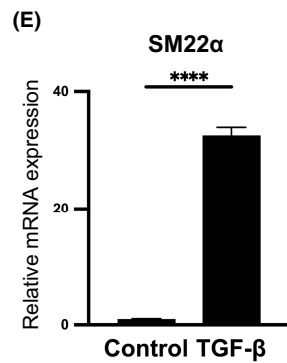
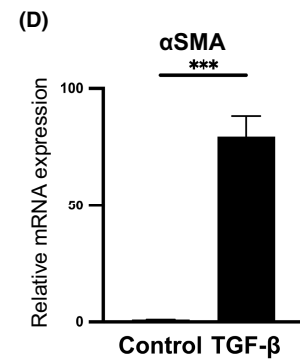
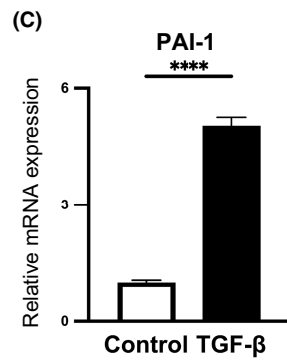
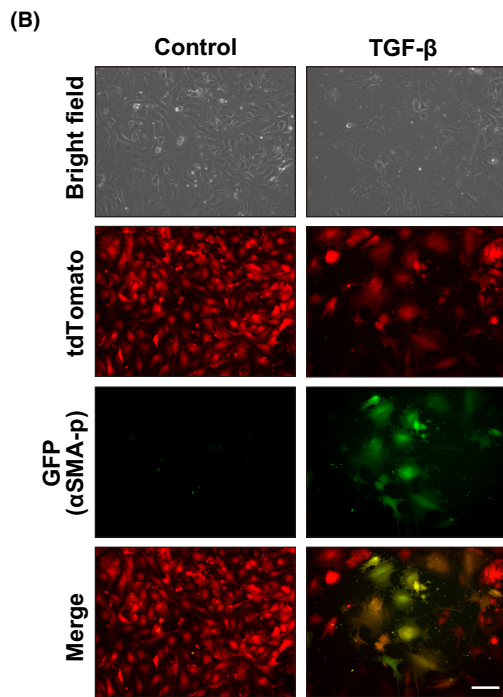
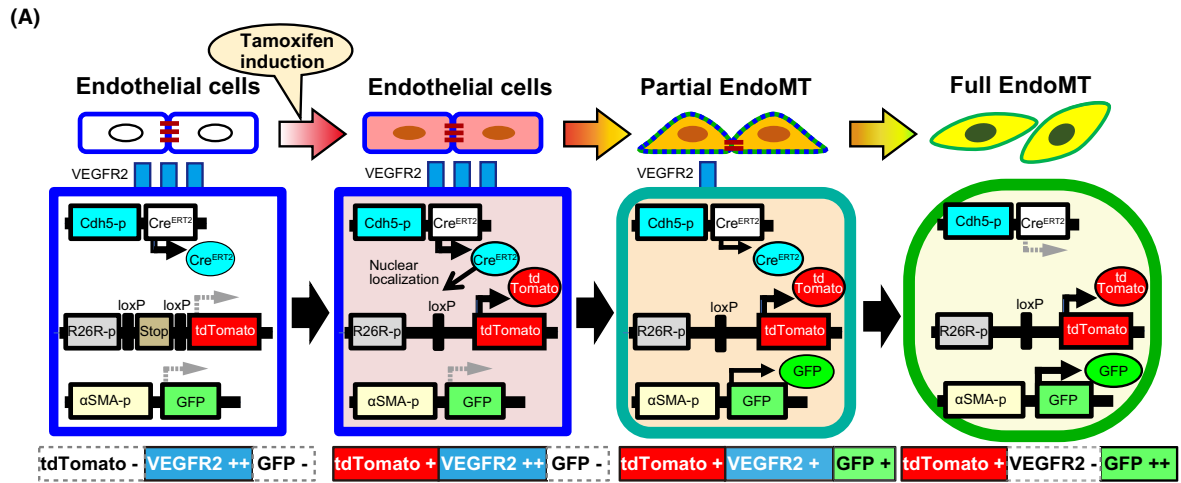


**FIGURE 2** Effects of TGF- $\beta$  on EndoMT reporter endothelial cells (EMRECs). (A) Schematic representation of EndoMT reporter system developed in this study. Cdh5-p, VE-cadherin promoter; Cre<sup>ERT2</sup>, Cre<sup>ERT2</sup> recombinase; R26R-p, R26Rosa promoter; LoxP, sites recognized by Cre recombinase;  $\alpha$ SMA-p,  $\alpha$ SMA promoter. (B–H) EMRECs treated without (Control) or with TGF- $\beta$  (5 ng/mL) for 24 h (C) or 72 h (B, D–H). (B) Bright field images and fluorescence signals corresponding to tdTomato (endothelial origin; red) and GFP (green) are shown. (C–F) Relative expression of a gene activated by TGF- $\beta$  signaling, PAI-1 (C), mesenchymal cell markers,  $\alpha$ SMA (D), and SM22 $\alpha$  (E) and an endothelial cell marker, VEGFR2 (F). All data are normalized to the  $\beta$ -actin expression. (G) Immunocytochemical analysis of EMRECs treated without (Control) or with TGF- $\beta$  (5 ng/mL). Fluorescence signals and immunostaining for tdTomato (red), GFP (green) VEGFR2 (cyan), and nuclei (blue) are shown. (H) Migration assay of EMRECs. Representative images of migrated cells and the quantitative analysis. Scale bars, 100  $\mu$ m (B, H) and 50  $\mu$ m (G). Statistical analyses: two-tailed unpaired Student's *t*-test; \*\*\**p* < 0.001; \*\*\*\**p* < 0.0001.

(Sigma-Aldrich, St. Louis, MO, USA) and Reconstitution Buffer (Nitta Gelatin), 8:1:1 (v/v/v). A 1% BSA-coated acupuncture  $\Phi$ 200-needle (No. 02, 0.20  $\times$  30 mm<sup>2</sup>, J type; Seirin, Shizuoka, Japan) was inserted to form a channel in the collagen gel, and the device was incubated at 37°C for 90 min. The needle was gently removed, and the luminal surface of the channel in the collagen gel was coated with 1 mg/mL fibronectin, followed by injection of the EMREC suspension (1.0  $\times$  10<sup>7</sup> cells/mL). The EMRECs were allowed to attach to the luminal surface at 37°C for 90 min in a humidified incubator. The device was then filled with culture medium, and the cells were cultured overnight to allow microvessel formation. The microvessels were treated with or without TGF- $\beta$ 2 for 72 h and subjected to immunocytochemical analyses and permeability assay as described in “Supporting Information”.

## 2.4 | Flow cytometry analysis and cell sorting

EMRECs cultured on RepCell culture dishes (CellSeed Inc., Tokyo, Japan) were treated without or with TGF- $\beta$ 2 for 68 h and collected with accutase (Innovative Cell Technologies, San Diego, CA, USA) in ice-cold Cell Dissociation Buffer (Thermo Fisher Scientific) containing 3 mM EDTA. EMRECs were then fixed with 2% paraformaldehyde (PFA) and incubated with allophycocyanin (APC)-conjugated anti-CD309 (VEGFR2) antibody, Brilliant Violet 421 (BV421)-conjugated anti-CD40 antibody or each fluorescent-conjugated isotype IgGs (Table S2). VEGFR2, CD40, and GFP were analyzed with flow cytometry using the ID7000 Spectral Cell Analyzer (SONY, Tokyo, Japan) and FlowJo software (BD Biosciences, Franklin Lakes, NJ, USA).

The cell sorting was carried out using a MoFlo XDP Flow Cytometer (Beckman Coulter, Brea, CA, USA). The cells were collected into medium containing 2% FBS and RNase inhibitor. The sorted cells were then subjected to qRT-PCR and bulk RNA-seq analyses, as described in “Supporting Information”.

## 2.5 | Statistical analysis

Significant differences between means were determined using two-tailed unpaired Student's *t*-test, one-way ANOVA with Tukey's multiple comparisons test, or Bonferroni's multiple comparisons test using Prism 10 software version 10.1.0 (GraphPad Software, Boston, MA, USA). Values are presented as mean  $\pm$  SD. Differences

between means were considered statistically significant at *p* < 0.05. The significance of gene sets from gene set enrichment analysis (GSEA) was based on normalized enrichment scores (NES) and nominal *p*-values.

Other procedures are described in “Appendix S1,” Supporting Materials and Methods.

## 3 | RESULTS

### 3.1 | Inhibition of TGF- $\beta$ signaling suppresses EndoMT in the TME

Multiple lines of evidence have shown that TGF- $\beta$  plays critical roles in tumor progression and metastasis through induction of EndoMT.<sup>9</sup> To verify in vivo induction of EndoMT by TGF- $\beta$  signaling, we used a mouse subcutaneous transplantation model of SAS cells, human OSCC. Immunostaining of human OSCC cell-derived tumor tissues identified the cells co-expressing platelet and endothelial cell adhesion molecule-1 (PECAM-1) and  $\alpha$ SMA, which are markers for endothelial and mesenchymal cells, respectively (Figure 1), suggesting that some endothelial cells in tumors underwent EndoMT.

We have previously developed a chimeric Fc receptor for TGF- $\beta$  ligands (extracellular domains of TGF- $\beta$  receptors fused with the Fc domain of immunoglobulin [IgG]: T $\beta$ RI-T $\beta$ RII-Fc), which traps all TGF- $\beta$  isoforms and inhibits TGF- $\beta$  signaling.<sup>20,21</sup> When recombinant T $\beta$ RI-T $\beta$ RII-Fc protein was administered to mice bearing oral cancer cell-derived tumors, to inhibit TGF- $\beta$  signaling in the TME,<sup>22</sup> the ratio of  $\alpha$ SMA in PECAM-1-positive cells in T $\beta$ RI-T $\beta$ RII-Fc-treated tumors was significantly lower than that in Control-Fc (human IgG-Fc)-treated tumors (Figure 1). In tumor vessels undergoing EndoMT,  $\alpha$ SMA is expressed not only in the endothelial cells undergoing EndoMT but also in pericytes.<sup>23</sup> Pericytes express neural/glial antigen 2 (NG2), which is widely considered as a pericyte marker.<sup>23</sup> Therefore, we performed staining with anti-NG2,  $\alpha$ SMA, and PECAM-1 antibodies. We found that cells expressing  $\alpha$ SMA overlapping with PECAM-1-positive area consist of NG2-positive and NG2-negative cells (Figure S1); thus, we defined the  $\alpha$ SMA-positive and NG2-negative cells detected among PECAM1-positive cells as cells that have undergone EndoMT. As shown in Figure S1, the ratio of such EndoMT cells decreased due to the inhibition of TGF- $\beta$  signals upon T $\beta$ RI-T $\beta$ RII-Fc treatment. These results suggest that inhibition of TGF- $\beta$  signaling suppresses EndoMT in oral cancer cell-derived tumors.

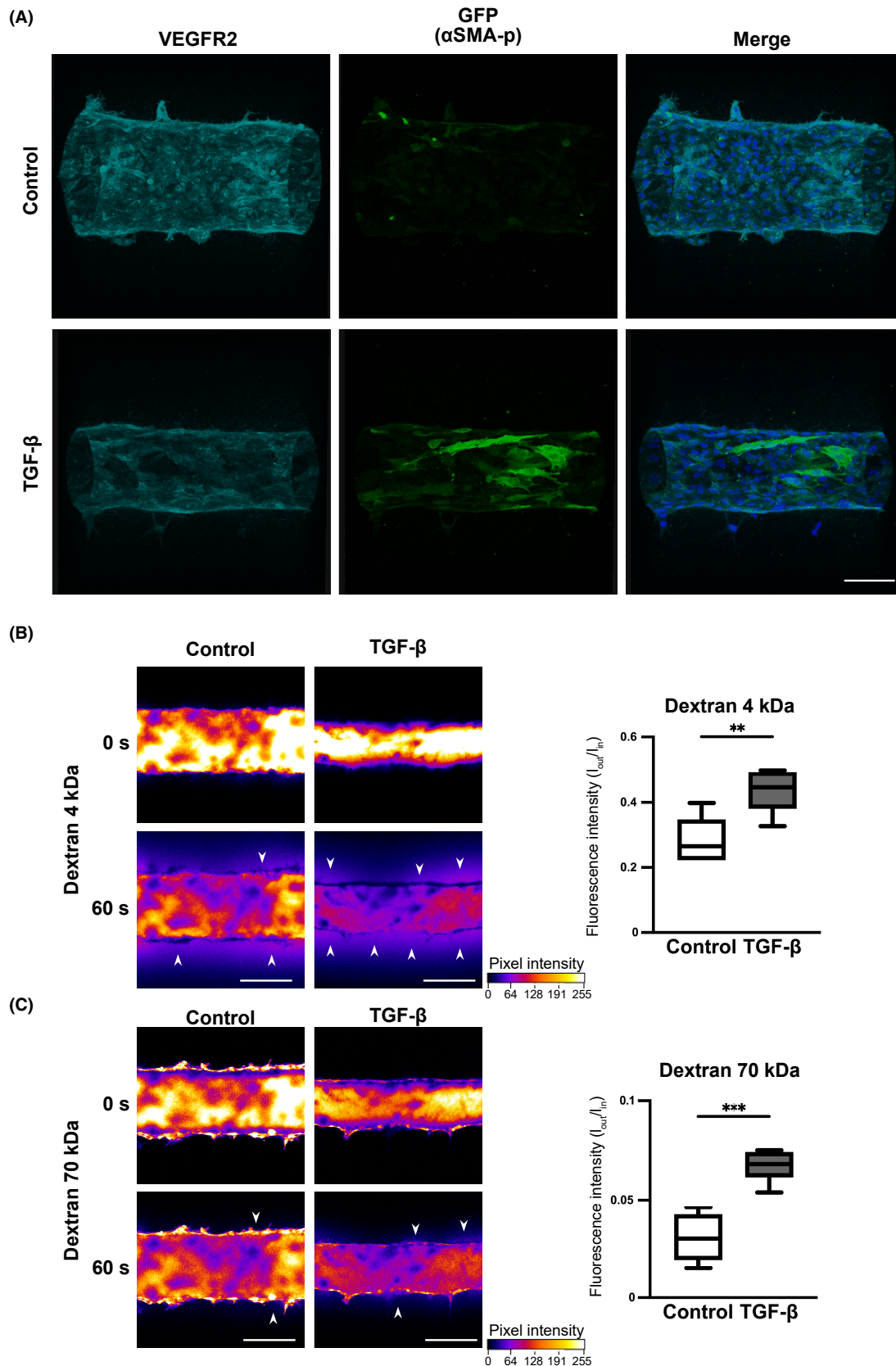


**FIGURE 3** TGF- $\beta$  stimulation induces EndoMT in EMREC-derived three-dimensional (3D) microvessel. (A–C) Microvessels formed by EMRECs in a collagen gel were treated without (Control) or with TGF- $\beta$  (5 ng/mL) for 72 h. (A) The immunostaining corresponding to VEGFR2 (cyan), GFP (green), and nuclei (blue) is shown. (B, C) Permeability assay using 4 kDa FITC-dextran (B) and 70 kDa TRITC-dextran (C). Fluorescence micrographs showing diffusion of dextran into collagen gel under designated conditions and quantitative analysis. Scale bars: 100  $\mu$ m (A) and 200  $\mu$ m (B, C). Statistical analyses: two-tailed unpaired Student's *t*-test; \*\**p* < 0.01; \*\*\**p* < 0.001.

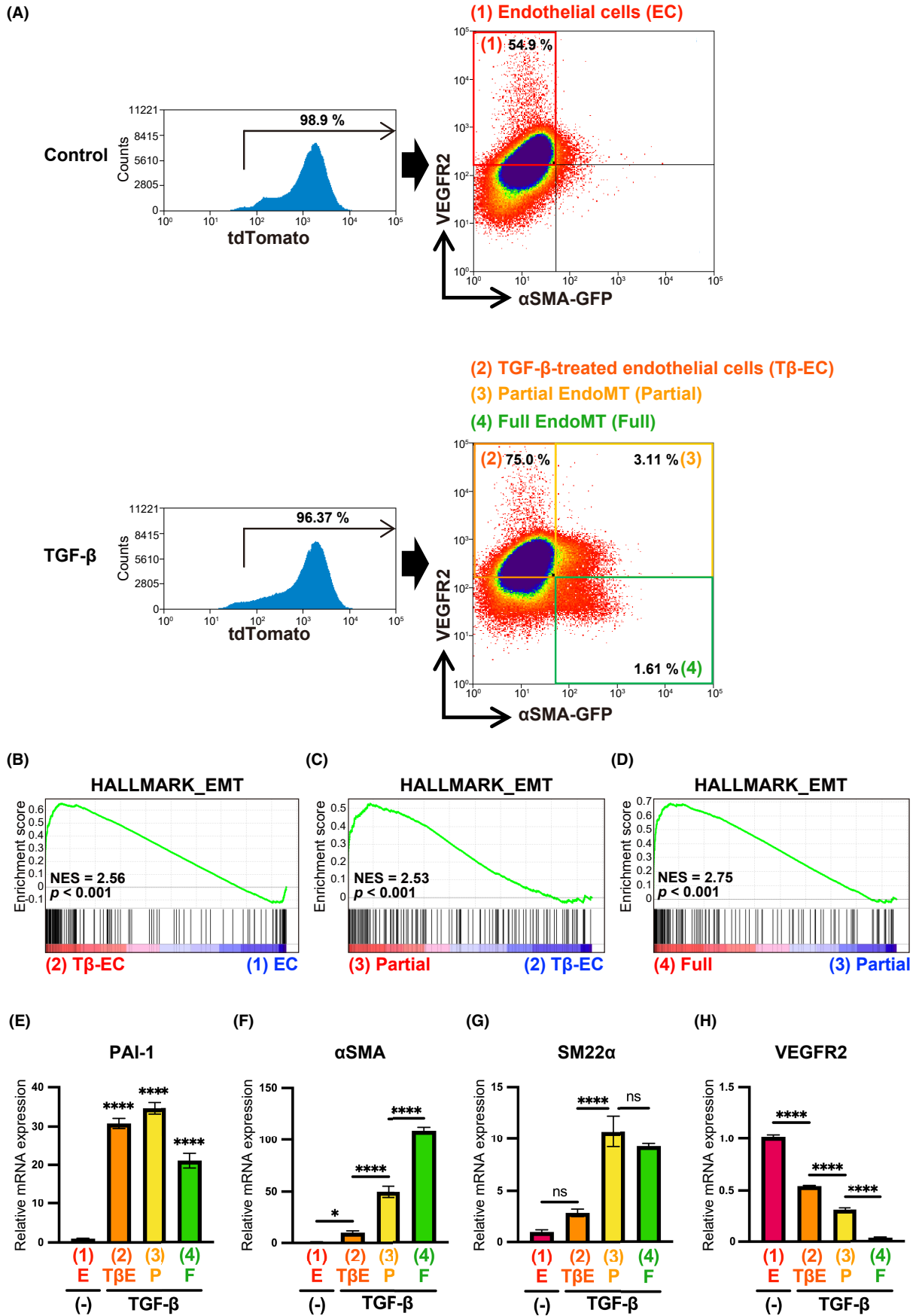


FIGURE 4 Legend on next page

**FIGURE 4** EMRECs visualize gradual changes of EndoMT, from endothelial cells, through partial EndoMT to full EndoMT state. (A) Sorting strategy of EMRECs treated without (Control; [-]) or with TGF- $\beta$  (5 ng/mL) for 68 h, based on the fluorescence signal related to tdTomato, GFP, and staining for VEGFR2. The tdTomato-negative cells were excluded from the main population (left panels). VEGFR2-positive and  $\alpha$ SMA-GFP-negative cells (left upper gated area in right panels: [1] or [2]), VEGFR2-positive, and  $\alpha$ SMA-GFP-positive cells (right upper gated area in bottom right panel: [3]). VEGFR2-negative and  $\alpha$ SMA-GFP-positive cells (right lower gated area in bottom right panel: [4]) were collected and used for further experiments. The collected cell fractions were termed endothelial cells ([1] EC), TGF- $\beta$ -treated endothelial cells ([2] T $\beta$ -EC), partial EndoMT cells ([3] Partial), and full EndoMT cells ([4] Full). (B–D) gene set enrichment analysis (GSEA) for the hallmark EMT, comparing bulk RNA-seq data from sorted fractions. NES, normalized enrichment score. *p*, nominal *p*-value. (F–H) Relative expression of PAI-1 (E),  $\alpha$ SMA (F), SM22 $\alpha$  (G), and VEGFR2 (H) in EC, T $\beta$ -EC (T $\beta$ E), Partial (P) and Full (F) fractions. All data are normalized to the  $\beta$ -actin expression. Statistical analyses: One-way ANOVA; \**p* < 0.05; \*\*\*\**p* < 0.0001; ns, not significant.

### 3.2 | Establishment of EndoMT reporter endothelial cells (EMRECs)

We have previously reported that TGF- $\beta$  induces EndoMT in multiple types of human and murine endothelial cells<sup>10,24–26</sup>; however, cells in partial EndoMT were not identified. To visualize the stepwise changes during EndoMT, we utilized genetic labeling of endothelial cell lineage in combination with live imaging of mesenchymal cells by crossing a tamoxifen-inducible endothelial-specific Cre line, Cdh5-BAC-Cre<sup>ERT2</sup> (Cdh5-Cre<sup>ERT2</sup>) mice,<sup>27</sup> with R26Rosa-loxP-Stop-loxP-tdTomato (LSL-tdTomato) mice and mesenchymal-specific GFP reporter line that express GFP under control of  $\alpha$ SMA promoter,  $\alpha$ SMA-GFP mice (Figure 2A). Because Cdh5-Cre<sup>ERT2</sup> mice express Cre recombinase under the control of the endothelial cell-specific marker VE-cadherin (Cdh5) promoter, the tdTomato is expressed in cells derived from the endothelial cell lineage. In addition,  $\alpha$ SMA-GFP transgene marks the  $\alpha$ SMA-positive cells of mesenchymal origin as well as EndoMT-derived cells of endothelial origin. Therefore, endothelial cells that have undergone full EndoMT co-express tdTomato and GFP, but do not express endothelial cell markers such as VEGFR2 (Figure 2A). Notably, cells in partial EndoMT are expected to express tdTomato, GFP and VEGFR2.

To characterize the various processes during EndoMT, we isolated endothelial cells from the livers of transgenic mice and immortalized them to establish EMRECs, which express tdTomato (Figure 2B). When EMRECs were cultured in the presence of TGF- $\beta$ 2 (hereafter termed “TGF- $\beta$ ”) for 72 h, some EMRECs exhibited GFP expression, suggesting TGF- $\beta$ -mediated activation of  $\alpha$ SMA promoter (Figure 2B).

To examine the effects of TGF- $\beta$  on the expression of various EndoMT markers in EMRECs, we performed qRT-PCR and immunocytochemical analyses. TGF- $\beta$  upregulated the expression of PAI-1, a target gene of TGF- $\beta$  signaling (Figure 2C), suggesting that EMRECs respond to TGF- $\beta$ . TGF- $\beta$  also upregulated the expressions of mesenchymal cell markers  $\alpha$ SMA and SM22 $\alpha$  (Figure 2D,E). In contrast, the expressions of endothelial cell markers VEGFR2 and Tie2 decreased upon TGF- $\beta$  treatment (Figure 2F and Figure S2A). The effects of TGF- $\beta$  on the expression of VEGFR2 were also confirmed at protein level (Figure 2G). We also verified the effect of TGF- $\beta$  on

the RNA expression of various EndoMT markers in MS1, a mouse pancreas endothelial cell line (Figure S2B–F).

Previous reports have shown that endothelial cells acquire enhanced motility during EndoMT.<sup>8</sup> Chamber migration assay revealed that TGF- $\beta$  enhances the EMREC motility (Figure 2H), indicating that EMRECs undergo functional EndoMT in response to TGF- $\beta$  signaling.

### 3.3 | TGF- $\beta$ induces EndoMT in EMREC-derived 3D microvessels

As blood vessels form 3D luminal structures in vivo, the vascular structure must be mimicked in vitro to understand mechanisms underlying EndoMT in blood vessels. Therefore, to examine the effects of TGF- $\beta$ -induced EndoMT in blood vessels, we adapted our in vitro model technology to create 3D endothelium microvessels<sup>18,19</sup> using EMRECs. Incubation of EMREC-derived microvessels in the absence or presence of TGF- $\beta$  for 72 h followed by staining for VEGFR2, revealed decreased VEGFR2 expression throughout the microvessels upon TGF- $\beta$  treatment. In contrast,  $\alpha$ SMA-GFP expression was not uniform, was sparse, and was restricted to some EMRECs in the microvessels (Figure 3A and Movies S1 and S2). Moreover, the diameter of the microvessels was reduced by TGF- $\beta$  treatment (Figure S3A). We found that treatment of microvessels with TGF- $\beta$  reduced the ratio of proliferating cells characterized by Ki67-positive staining (Figure S3B,C). These results suggest that the decrease in the diameter of microvessels was caused by the inhibitory effects of TGF- $\beta$  on the proliferation of endothelial cells, as previously reported.<sup>26,28</sup>

Previous reports have shown that EndoMT impairs the barrier function of lymphatic vessels.<sup>29</sup> Permeability assay was performed by simultaneous injection of fluorescent-conjugated dextran probes (4 kDa and 70 kDa) in the lumen of microvessels.<sup>30</sup> The spatial redistribution of dextran probes was monitored by confocal microscopy for 60 s (Figure 3B,C). Both dextrans leaked from TGF- $\beta$ -treated microvessels into the collagen gel at higher levels when compared with control microvessels (Figure 3B,C), suggesting that TGF- $\beta$ -induced EndoMT impaired the barrier function of EMREC-derived microvessels. These results suggest that EMRECs exhibit various phenotypes of TGF- $\beta$ -induced EndoMT in 3D microvessels.



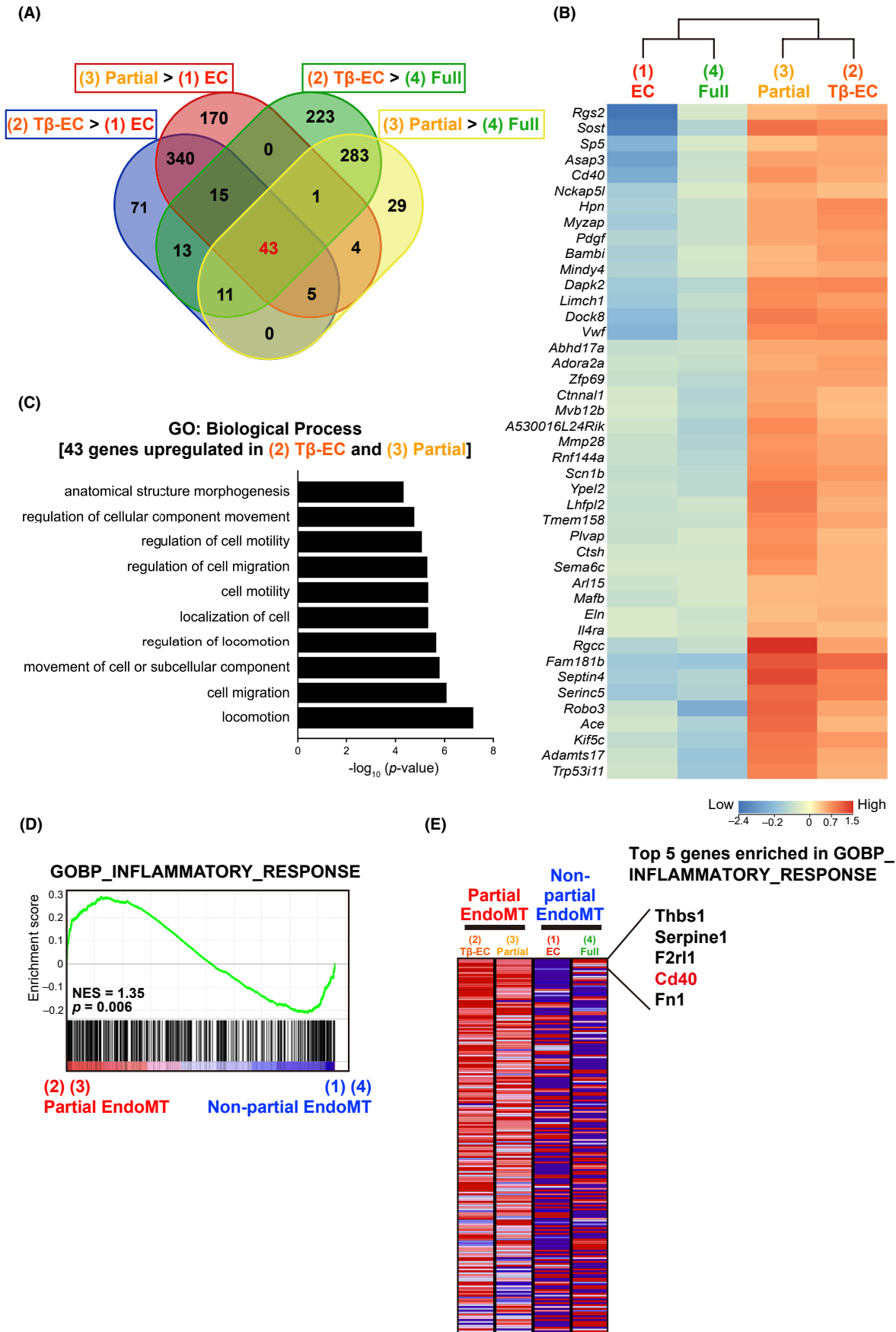


FIGURE 5 Legend on next page

**FIGURE 5** EMRECs enable identification of genes upregulated specifically in partial EndoMT state. (A) Venn diagram showing the number of total and overlapping genes upregulated under indicated conditions. (B) Heat map of the 43 genes upregulated in cells corresponding to T $\beta$ -EC and Partial fractions. High (red) and low (blue) levels of expression are indicated. (C) GO enrichment analysis of 43 genes upregulated in T $\beta$ -EC and Partial fractions. (D) Gene set enrichment analysis (GSEA) of the inflammatory response genes, comparing bulk RNA-seq data from partial EndoMT ([2] T $\beta$ -EC and [3] Partial) and non-partial EndoMT ([1] EC and [4] Full) fractions. NES, normalized enrichment score. *p*, nominal *p*-value. (E) Heat map of DEGs ranked by GSEA in the core of inflammatory response gene set using bulk RNA-seq data from partial EndoMT ([2] T $\beta$ -EC and [3] Partial) and non-partial EndoMT ([1] EC and [4] Full) fractions. High (red) and low (blue) levels of expression are indicated.

### 3.4 | Stepwise changes during EndoMT are observed in EMRECs

As EMRECs enabled us to visualize various changes in endothelial cells during TGF- $\beta$ -induced EndoMT, we next attempted to isolate multiple subpopulations of endothelial cells undergoing EndoMT using FACS. EMRECs were cultured in the absence or presence of TGF- $\beta$ , followed by FACS analysis. To establish EMRECs, we utilized genetic labeling of endothelial cell lineage; thus, all cells of endothelial origin should express tdTomato. To determine VEGFR2 and  $\alpha$ SMA-GFP expression in EMRECs, we analyzed tdTomato-positive cells, expressing tdTomato at a high level (tdTomato<sup>high</sup>), because they should not contain non-endothelial cells (Figure S4). While EMRECs scarcely expressed  $\alpha$ SMA-GFP, TGF- $\beta$  induced the emergence of  $\alpha$ SMA-GFP-positive EMRECs (Figure S4). Furthermore, we found that  $\alpha$ SMA-GFP-positive EMRECs comprised VEGFR2-positive and VEGFR2-negative subpopulations. The profiles obtained with tdTomato<sup>high</sup> cells were similar to the profiles obtained with the whole tdTomato-positive cell population (Figure 4A). Therefore, to isolate the multiple subpopulations of endothelial cells undergoing EndoMT and to collect large amounts of cells for further analysis, we targeted cells in all tdTomato-positive cells. We sorted VEGFR2-positive/ $\alpha$ SMA-GFP-negative cells from TGF- $\beta$ -untreated and TGF- $\beta$ -treated EMRECs (fractions [1] and [2], respectively; Figure 4A). We also sorted VEGFR2-positive/ $\alpha$ SMA-GFP-positive and VEGFR2-negative/ $\alpha$ SMA-GFP-positive cells from TGF- $\beta$ -treated EMRECs (fractions [3] and [4], respectively; Figure 4A). To evaluate the mesenchymal state of the sorted fractions, we performed bulk RNA-seq analysis. We compared the mesenchymal states of the four sorted fractions by GSEA using an EMT hallmark gene set and found that fraction (2) (TGF- $\beta$ -treated endothelial cells; hereafter termed "T $\beta$ -EC") exhibited stronger mesenchymal phenotypes than fraction (1) (TGF- $\beta$ -untreated endothelial cells; hereafter termed "EC") (Figure 4B). Moreover, fraction (3), which expressed both VEGFR2 and  $\alpha$ SMA-GFP, exhibited stronger and weaker mesenchymal phenotypes than fraction (2) and fraction (4), respectively (Figure 4C,D), suggesting that fraction (3) and fraction (4) represent the cells undergoing partial EndoMT (hereafter termed "Partial") and full EndoMT (hereafter termed "Full"), respectively (Figure 4A).

We examined the expression of various EndoMT-related markers in the sorted fractions using qRT-PCR. PAI-1 was upregulated in all

TGF- $\beta$ -stimulated fractions (Figure 4E), suggesting that activation of TGF- $\beta$  signals was retained during EndoMT. The expressions of mesenchymal cell markers,  $\alpha$ SMA and SM22 $\alpha$ , were upregulated during EndoMT progression (Figure 4F,G). In accordance with the results for mesenchymal cell markers, the expressions of endothelial markers, VEGFR2, Tie2, and VE-cadherin gradually decreased from the EC to the Full fraction (Figure 4H and Figure S5A,B).

Further analysis of bulk RNA-seq data revealed that gene expression profiles of T $\beta$ -EC and Partial fractions were similar (Figure S5C,D). The expression profile of T $\beta$ -EC was comparable with that of EC (Figure S5C,D). Gene ontology (GO) enrichment analysis of the differentially expressed genes (DEGs) showed that angiogenesis- and migration-related GO terms were enriched in T $\beta$ -EC, Partial, and Full fractions compared to those in EC (Figure S5E-G). GSEA revealed that EndoMT occurred gradually from EC to Full via T $\beta$ -EC and Partial fractions (Figure S5H,I). Notably, the expressions of the hallmark angiogenesis- and endothelial migration-related genes were upregulated in the T $\beta$ -EC and Partial fractions (Figure S5J-M). These results suggest that the cells in both T $\beta$ -EC and Partial fractions represent the populations of endothelial cells undergoing partial EndoMT.

### 3.5 | Identification of CD40 as a novel marker for partial EndoMT

To clarify the molecular characteristics of partial EndoMT, we attempted to identify genes upregulated in partial EndoMT. RNA-seq analysis identified 43 genes upregulated in cells representing partial EndoMT states (T $\beta$ -EC- and Partial-induced genes; Figure 5A,B and Table S3). GO enrichment analysis of the 43 genes revealed that they were involved in locomotion and cell migration (Figure 5C).

In accordance with our previous report that inflammation is involved in the induction of EndoMT,<sup>10</sup> GSEA revealed the enrichment of inflammatory response-related genes in T $\beta$ -EC and Partial fractions, suggesting that inflammatory response signaling is activated in cells undergoing partial EndoMT (Figure 5D). Therefore, we focused on inflammatory response-related genes. Among the top five enriched genes in the GSEA gene set related to the inflammatory response, we identified CD40 as a partial EndoMT-induced gene, which controls various immune and inflammatory responses (Figure 5E).

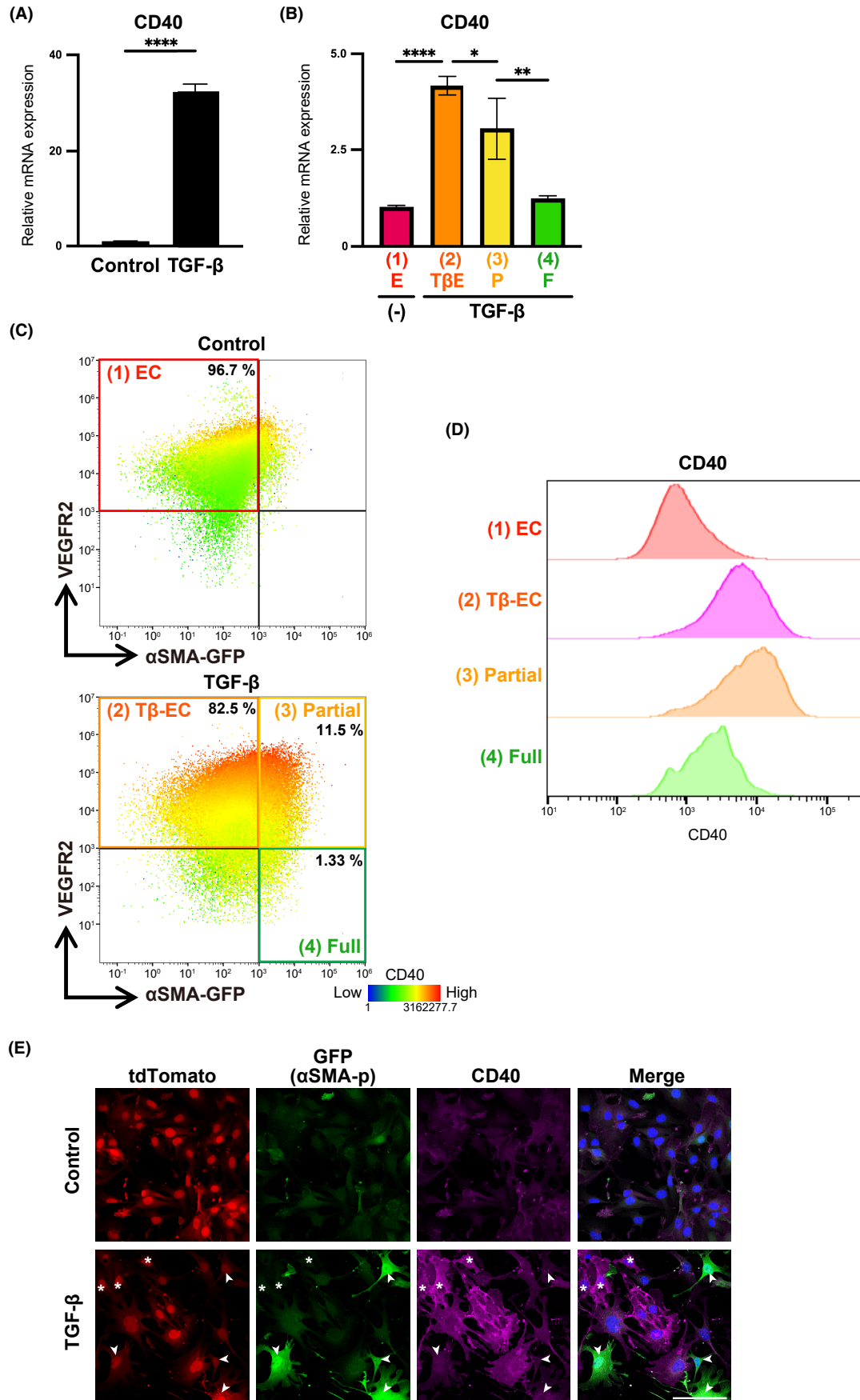


FIGURE 6 Legend on next page

**FIGURE 6** CD40 Expression is upregulated in partial EndoMT state. (A,B) Relative expression of CD40 in EMRECs treated without (Control) or with transforming growth factor- $\beta$  (TGF- $\beta$ ) (5 ng/mL) for 72 h (A) and in EC, T $\beta$ -EC, Partial and Full fractions (B). All data are normalized to the  $\beta$ -actin expression. (C, D) FACS analysis of EMRECs treated without (Control) or with TGF- $\beta$  (5 ng/mL) for 68 h. (C) Fluorescence signals and staining for VEGFR2 and CD40. High (red) and low (green) levels of CD40-staining are indicated. (D) Histograms showing the expression levels of CD40 in EC, T $\beta$ -EC, Partial, and Full fractions. (E) Fluorescence signals and immunostaining of EMRECs treated without (Control) or with TGF- $\beta$  (5 ng/mL) for 72 h, tdTomato (red), GFP (green), CD40 (magenta), and nuclei (blue) are shown. Arrowheads indicate  $\alpha$ SMA-GFP<sup>high</sup>/CD40<sup>low</sup> cells and asterisks indicate  $\alpha$ SMA-GFP<sup>low</sup>/CD40<sup>high</sup> cells. Scale bar, 100  $\mu$ m. Statistical analyses: two-tailed unpaired Student's *t*-test (A) and one-way ANOVA (B); \**p* < 0.05; \*\**p* < 0.01; \*\*\*\**p* < 0.0001.

### 3.6 | CD40 expression is enriched in partial EndoMT state and regulates the progression of EndoMT

Our data suggested that CD40 is a potential novel partial EndoMT-specific marker. CD40 is a member of the TNF-receptor superfamily<sup>31</sup> and its expression in endothelial cells can be upregulated in response to TNF- $\alpha$  and other cytokines.<sup>32</sup> In addition, CD40 contributes to inflammation-driven angiogenesis.<sup>33</sup> We observed that CD40 was upregulated in TGF- $\beta$ -treated EMRECs and MS1 cells (Figure 6A and Figure S6A). Moreover, CD40 mRNA and protein expression levels were upregulated in T $\beta$ -EC and Partial fractions compared to those in EC and Full fractions (Figure 6B–D and Figure S6B–D). Immunocytochemical analysis using anti-CD40 antibody revealed low  $\alpha$ SMA-GFP or CD40 expression in EMRECs cultured without TGF- $\beta$  (Figure 6E). Of note, we observed two subsets of TGF- $\beta$ -treated EMRECs with varied expression of  $\alpha$ SMA-GFP and CD40:  $\alpha$ SMA-GFP<sup>low</sup>/CD40<sup>high</sup> and  $\alpha$ SMA-GFP<sup>high</sup>/CD40<sup>low</sup> (Figure 6E). Because CD40 and  $\alpha$ SMA-GFP are considered as markers for partial and full EndoMT, respectively, we concluded that the first and second subsets of EMRECs represented the population of cells undergoing partial and full EndoMT, respectively.

To examine the roles of CD40 in TGF- $\beta$ -induced EndoMT, we used siRNAs specific for CD40 to suppress the expression of CD40 in EMRECs treated with TGF- $\beta$ . CD40-specific siRNAs effectively inhibited CD40 expression (Figure 7A) and enhanced TGF- $\beta$ -induced expressions of  $\alpha$ SMA and SM22 $\alpha$  in comparison to TGF- $\beta$  treated ECs (Figure 7B,C), suggesting that CD40 might regulate EndoMT progression.

### 3.7 | Single-cell RNA sequencing of human tumors revealed that CD40 is expressed in the endothelial cells undergoing partial EndoMT

Next, we examined the clinical significance of our *in vitro* findings using scRNA-seq data from human tumors. We previously performed pan-cancer analysis on 226 samples across 10 solid cancer types to examine the TME profile at single-cell resolution.<sup>31</sup> To identify the subpopulations of cells undergoing partial EndoMT in TME, we used the same scRNA-seq data, clustered the cells by principal component analysis and characterized the subpopulations of cells with the gene expression profiles of endothelial cells (clusters 1–3) and CAFs (clusters 3–6) (Figure 8A and Figure S7A–D).

Violin plot analyses showed that the expression of endothelial cell markers PECAM-1 and von Willebrand factor (vWF) was associated with EC clusters, while the expression of mesenchymal cell markers Collagen1A1 and  $\alpha$ SMA was associated with CAF clusters (Figure 8B–E and Figure S7A–D). We also found that both endothelial and mesenchymal cell markers were expressed in cluster 3, suggesting that cluster 3 represented cells undergoing partial EndoMT (Figure 8A–E and Figure S7A–D). Remarkably, CD40 was expressed in cluster 3 (Figure 8F and Figure S7E).

Subsequently, to characterize the functional heterogeneities in pan-cancer cells, we defined a pseudotime for each cell along an elastic principal tree, computed by Monocle functions.<sup>35</sup> The pseudotime analysis revealed that the trajectory for EndoMT began at the EC clusters, with the fractions of cells progressing into partial EndoMT cluster and finally into CAF clusters (Figures 8G,H). These results indicate that human tumor tissues contain subpopulations of endothelial cells, as well as cells undergoing partial and full EndoMT and confirm that CD40 can be considered as a partial EndoMT marker in human tumors.

## 4 | DISCUSSION

In this study, we established EMRECs to visualize the sequential changes during EndoMT. Using EMRECs, we found that TGF- $\beta$  induced a sequential transition of endothelial cells from the early stage of partial EndoMT (T $\beta$ -EC) through to the late stage of partial EndoMT (Partial) to full EndoMT (Figures 4 and 9). As partial EndoMT is a stage in which the expressions of endothelial and mesenchymal cell markers change dynamically, these findings might serve as a valuable resource for elucidating the molecular mechanism that governs induction of EndoMT.

TGF- $\beta$  signals have been implicated in EndoMT induction, which was confirmed *in vitro* and *in vivo*. We also showed that TGF- $\beta$  induced partial EndoMT activated inflammatory signaling in EMRECs (Figure 5). We previously reported that inflammatory signals enhance TGF- $\beta$ -induced EndoMT.<sup>10,29</sup> Inflammatory signals have been implicated in the decreased endothelial barrier function following induction of EndoMT.<sup>36,37</sup> In the present study, we found that TGF- $\beta$ -induced EndoMT increased the permeability of 3D microvessels (Figure 3B). This effect likely resulted from the decreased barrier function and altered maturity of microvessels, as revealed by the decreased expression of VE-cadherin (Figure S5B). Our data suggested that CD40, a molecule involved in inflammatory responses, can be

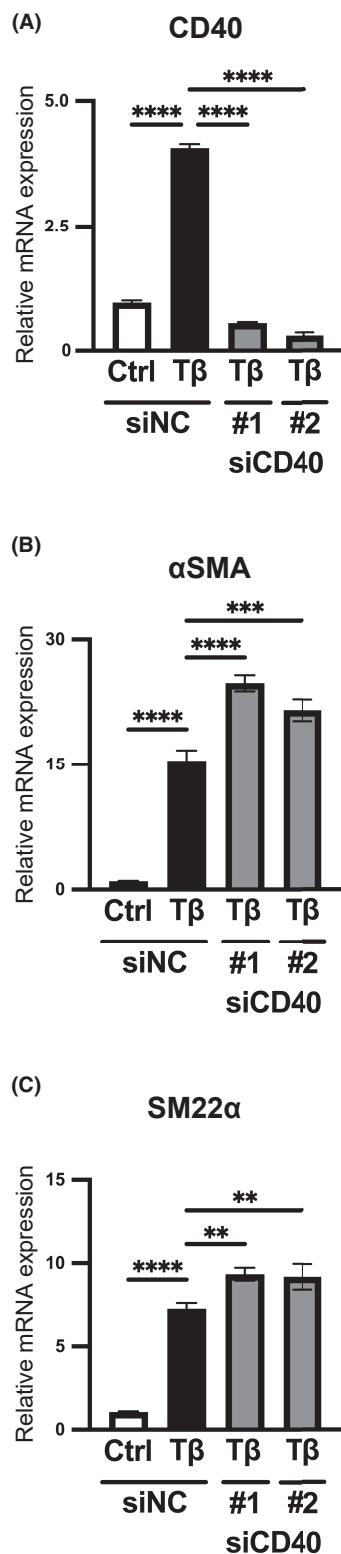


**FIGURE 7** Silencing CD40 enhances TGF- $\beta$ -induced EndoMT. EMRECs transfected with negative control siRNA (siNC) or siRNAs for CD40 (siCD40 #1 and #2) were treated without (Ctrl) or with TGF- $\beta$  (T $\beta$ ) (0.5 ng/mL) for 72 h. Relative expression of CD40 (A),  $\alpha$ SMA (B) and SM22 $\alpha$  (C) are shown. All data are normalized to the  $\beta$ -actin expression. Statistical analyses: one-way ANOVA; \*\* $p < 0.01$ ; \*\*\* $p < 0.001$ ; \*\*\*\* $p < 0.0001$ .

considered a partial EndoMT marker (Figures 5 and 6). CD40 is a member of the TNF-receptor superfamily and expressed on antigen-presenting cells such as B cells, dendritic cells, macrophages,<sup>31</sup> as well as on vascular endothelial cells.<sup>32</sup> Inflammatory cytokines such as TNF- $\alpha$  increase CD40 expression, contributing to inflammation-induced angiogenesis.<sup>33</sup> Activation of CD40 signaling depends on CD40 ligand (CD40L) presentation and is involved in various processes, including leukocyte recruitment and extravasation.<sup>38</sup> In addition, CD40-CD40L might be responsible for the induction of EndoMT in embryonic endothelial cells during chicken embryo development,<sup>39</sup> however, a direct association has not been addressed. Although the involvement of CD40 in EndoMT has been suggested, no studies have shown a direct correlation between CD40 and EndoMT or partial EndoMT under pathological conditions. In this study, we show for the first time that CD40 can be considered a partial EndoMT-specific marker (Figure 6). Furthermore, our data revealed that TGF- $\beta$ -induced EndoMT was enhanced upon CD40 silencing in EMRECs (Figure 7), suggesting that TGF- $\beta$ -induced CD40 expression suppressed the transition from partial EndoMT to full EndoMT. Our data also revealed that CD40 expression is upregulated by TGF- $\beta$  and associated with the population of TGF- $\beta$ -treated endothelial cells and cells undergoing partial EndoMT but downregulated in endothelial cells and cells undergoing full EndoMT.

We have previously demonstrated the presence of heterogeneous CAFs including EndoMT CAFs in human tumors.<sup>34</sup> The evolutionary trajectory suggested that such EndoMT CAFs represent the transitional state between tumor endothelial cells and myofibroblastic CAFs.<sup>34</sup> In this study, we identified a cluster of cells undergoing partial EndoMT (Figure 8), which likely represents the EndoMT CAFs,<sup>34</sup> using the same human tumor samples. However, further analysis is needed to determine the correlation between previously identified EndoMT CAFs and the partial EndoMT clusters. Furthermore, scRNA-seq analysis revealed that CD40 expression in human tumor tissues was enriched in a population of cells undergoing partial EndoMT (Figure 8). EndoMT is closely associated with tumor progression through the formation of CAFs and angiogenesis. Moreover, recent reports suggest that cells that underwent full EndoMT cannot reverse to endothelial cells, while partial EndoMT state is reversible allowing cells to regain their endothelial characteristics.<sup>9</sup> CAFs are originated from the cells that have undergone full EndoMT.<sup>9</sup> Thus, it is crucial to understand the mechanisms controlling the transition from partial EndoMT to full EndoMT to prevent the formation of CAFs. Because CD40 was shown to be expressed in the cells in partial EndoMT state, our data suggest that it may suppress the transition of cells to full EndoMT state. In addition, our findings indicate that CD40 might be considered as a useful partial EndoMT marker for diagnosing and treating cancer progression and metastasis (Figure 9).

Multiple lines of evidence suggest that EMT transcription factors (EMT-TFs) such as Snail and ZEB1 play important roles not only in the induction of EMT but also EndoMT.<sup>40</sup> The exact roles of EMT-TFs in the sequential steps of EndoMT need to be elucidated

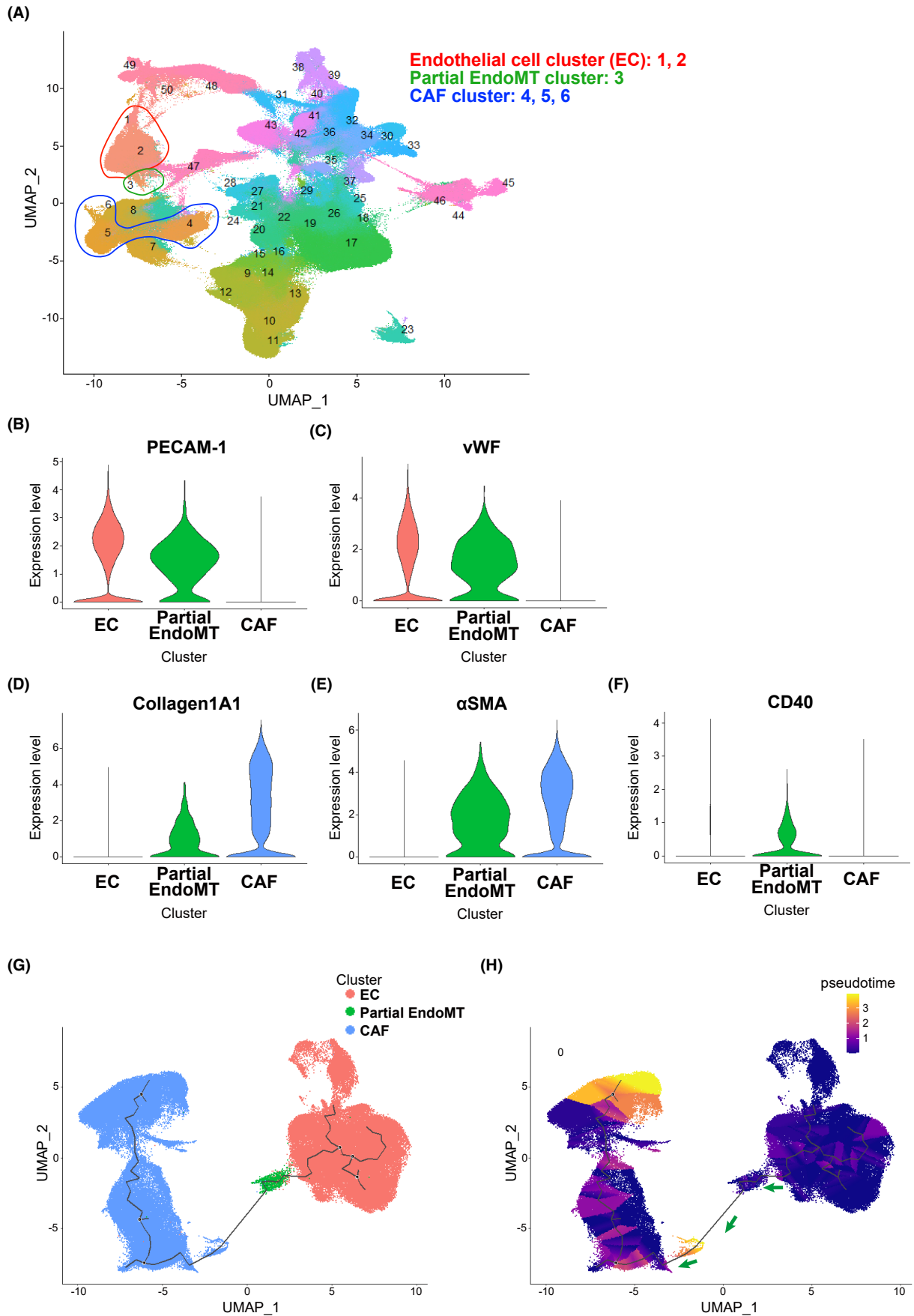


**FIGURE 8** A scRNA-seq identifies a subset of cells associated with partial EndoMT in human tumors. (A) Visualization of single-cell transcriptome with Uniform Manifold Approximation and Projection (UMAP). Projection of 855,271 cells derived from 226 patients bearing 10 types of common solid tumors<sup>34</sup> and clustering results. Clusters 1 and 2 enclosed by a red line represent endothelial cells, cluster 3 enclosed by a green line represents cells in partial EndoMT state and clusters 4–6 enclosed by a blue line represent CAFs. (B–F) Violin plots showing the distribution of the expression of PECAM-1 (B), vWF (C), Collagen1A1 (D),  $\alpha$ SMA (E), and CD40 (F) across the EC, partial EndoMT and CAF clusters. (G, H) Single-cell trajectory analysis of EndoMT represented by elastic principal tree showing a progression from EC to CAF clusters (green arrows).

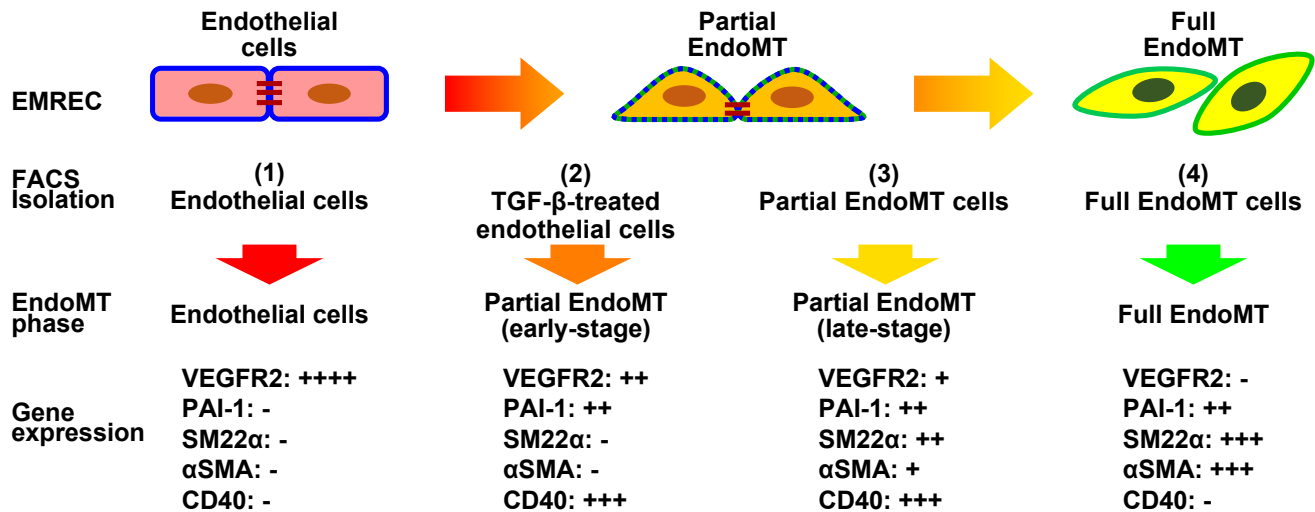


**FIGURE 9** The stepwise changes during endothelial-mesenchymal transition (EndoMT). During EndoMT, endothelial cells transdifferentiate to full EndoMT cells through partial EndoMT. EndoMT reporter endothelial cells (EMRECs) revealed that partial EndoMT has two stages: early and late. It also enabled the identification of CD40 as a novel partial EndoMT marker. In the cells undergoing early stage of partial EndoMT, the expressions of endothelial cell markers are lower than that in endothelial cells. Concomitantly, the mesenchymal cell marker level is low, but CD40 expression is upregulated. When the transition proceeds to the late stage of partial EndoMT, endothelial cell marker expression decreases less than that in the early stage of partial EndoMT, but is higher than that in cells undergoing full EndoMT. Simultaneously, mesenchymal cell marker expression is higher than that in the early stage of partial EndoMT, but still lower than that in the cells representing full EndoMT. Importantly, even during the transition from the early stage to the late stage of partial EndoMT, the expression of newly identified partial EndoMT marker, CD40, is high but reduced in the cells representing full EndoMT state.

in the future. EndoMT is involved in not only tumor progression but also in various diseases such as atherosclerosis, pulmonary arterial hypertension, cardiac fibrosis, and organ fibrosis.<sup>8,9</sup> The EMRECs (Figure 2) and 3D microvessel model (Figure 3) established in this study can be used to evaluate the dynamics and distribution of EndoMT in pathological conditions. EMRECs can be also applied to study the efficacy of therapeutic agents by live imaging in a system mimicking the in vivo environment. In addition, imaging technology using EMRECs might be used to screen novel therapeutic drugs targeting each EndoMT stage.

#### AUTHOR CONTRIBUTIONS

**Kazuki Takahashi:** Conceptualization; data curation; formal analysis; funding acquisition; investigation; methodology; supervision; writing – original draft; writing – review and editing. **Miho Kobayashi:** Conceptualization; data curation; formal analysis; funding acquisition; investigation; methodology; supervision; writing – original draft; writing – review and editing. **Hisae Katsumata:** Investigation; writing – review and editing. **Shiori**

**Tokizaki:** Funding acquisition; investigation; writing – review and editing. **Tatsuhiko Anzai:** Data curation; formal analysis; investigation; methodology; writing – original draft; writing – review and editing. **Yukinori Ikeda:** Investigation; writing – review and editing. **Daniel M. Alcaide:** Investigation; writing – review and editing. **Kentaro Maeda:** Investigation; writing – review and editing. **Makoto Ishihara:** Data curation; formal analysis; investigation; writing – review and editing. **Katsutoshi Tahara:** Data curation; formal analysis; investigation; writing – review and editing. **Yoshiaki Kubota:** Data curation; formal analysis; writing – review and editing. **Fumiko Itoh:** Investigation; writing – review and editing. **Jihwan Park:** Data curation; formal analysis; writing – review and editing. **Kunihiko Takahashi:** Supervision; writing – review and editing. **Yukiko T. Matsunaga:** Data curation; formal analysis; supervision; writing – review and editing. **Yasuhiro Yoshimatsu:** Conceptualization; data curation; formal analysis; funding acquisition; methodology; supervision; writing – review and editing. **Katarzyna A. Podyma-Inoue:** Data curation; formal analysis; funding acquisition; methodology; writing – original draft; writing

– review and editing. **Tetsuro Watabe**: Conceptualization; data curation; formal analysis; funding acquisition; methodology; supervision; writing – original draft; writing – review and editing.

## ACKNOWLEDGMENTS

The authors are grateful to Dr. Katsuhito Fujiu (the University of Tokyo, Japan) for providing  $\alpha$ SMA-GFP mice and to Dr. Mikako Shirouzu and Dr. Takehisa Matsumoto (RIKEN, Japan) for preparation of Fc chimeric proteins. The authors would also like to thank Mizuki Tanaka (TMDU), Eri Otsuka (the University of Tokyo), and Jia Kim (Tokyo University of Pharmacy and Life Sciences) for technical assistance, Dr. Kohei Miyazono (the University of Tokyo) and the members of Department of Biochemistry, TMDU for critical discussion. Immunocytochemical analysis was performed at the Research Core of TMDU. The super-computing resource was provided by Human Genome Center, the University of Tokyo.

## FUNDING INFORMATION

This work was supported by research programs of the Japan Agency for Medical Research and Development (AMED) (grant nos. JP21cm0106253 and JP22ama221205 to T.W.). The present study was also supported in part by the Grant-in-Aid for Scientific Research (B) (grant no. JP20H03851 to T.W.), Scientific Research (C) (grant nos. JP15K21394 to Y.Y., JP19K07674 to M.K. and JP20K10111 to K.A.P.I.), Grant-in-Aid for Early-Career Scientist (grant no. JP23K15962 to Ka.Tak.), and JSPS Fellow (grant nos. JP20J11926 and JP21J01294 to Ka.Tak.) from the Japan Society for the Promotion of Science (JSPS), the Health Sciences Research (grant no. 21KD2004 to T.W.), JST SPRING (JPMJSP2120 to S.T.), and Nanken-Kyoten, TMDU. This work was also supported by the Cooperation Program between TMDU, Sony Corporation, and Sony Group Corporation.

## CONFLICT OF INTEREST STATEMENT

M.I. and K.Tah. are employees of Sony Corporation. T.W. has received research funding from Sony Corporation. T.W. is an Editorial Board member of *Cancer Science*. All other authors declare that they have no competing interests.

## ETHICS STATEMENT

Approval of the research protocol by an Institutional Reviewer Board: The experimental procedures for plasmid construction were approved by the Genetically Modified Organisms Safety Committee of Tokyo Medical and Dental University (registration number: G2019-026C6) and by the President of Tokyo University of Pharmacy and Life Sciences (registration number: LSR3-015).

Informed Consent: N/A.

Registry and the Registration No. of the study/trial: N/A.


Animal Studies: The animal experiment procedures were approved by the Institutional Animal Care and Use Committee at Tokyo University of Pharmacy and Life Sciences (approval number: L16-13, LS27-007) and the Institutional Animal Care and Use Committee of

Tokyo Medical and Dental University (registration number: A2021-133C5) and were performed according to the guidelines of both institutions.

## ORCID

Miho Kobayashi  <https://orcid.org/0000-0003-2548-4120>

Fumiko Itoh  <https://orcid.org/0000-0002-6134-5331>

Katarzyna A. Podyma-Inoue  <https://orcid.org/0009-0001-9720-0898>

[org/0009-0001-9720-0898](https://orcid.org/0009-0001-9720-0898)

Tetsuro Watabe  <https://orcid.org/0000-0001-5836-1309>

## REFERENCES

- Hanahan D, Weinberg RA. Hallmarks of cancer: the next generation. *Cell*. 2011;144:646-674.
- Oikawa Y, Michi Y, Tsushima F, et al. Management of retropharyngeal lymph node metastasis in oral cancer. *Oral Oncol*. 2019;99:104471.
- Miyazono K, Katsuno Y, Koinuma D, Ehata S, Morikawa M. Intracellular and extracellular TGF- $\beta$  signaling in cancer: some recent topics. *Front Med*. 2018;12:387-411.
- Derynck R, Budi EH. Specificity, versatility, and control of TGF- $\beta$  family signaling. *Sci Signal*. 2019;12:eaav5183.
- Pickup M, Novitskiy S, Moses HL. The roles of TGF $\beta$  in the tumour microenvironment. *Nat Rev Cancer*. 2013;13:788-799.
- Liu S, Ren J, Ten Dijke P. Targeting TGF $\beta$  signal transduction for cancer therapy. *Signal Transduct Target Ther*. 2021;6:8.
- Derynck R, Turley SJ, Akhurst RJ. TGF $\beta$  biology in cancer progression and immunotherapy. *Nat Rev Clin Oncol*. 2021;18:9-34.
- Yoshimatsu Y, Watabe T. Emerging roles of inflammation-mediated endothelial-mesenchymal transition in health and disease. *Inflamm Regen*. 2022;42:9.
- Watabe T, Takahashi K, Pietras K, Yoshimatsu Y. Roles of TGF- $\beta$  signals in tumor microenvironment via regulation of the formation and plasticity of vascular system. *Semin Cancer Biol*. 2023;92:130-138.
- Yoshimatsu Y, Wakabayashi I, Kimuro S, et al. TNF- $\alpha$  enhances TGF- $\beta$ -induced endothelial-to-mesenchymal transition via TGF- $\beta$  signal augmentation. *Cancer Sci*. 2020;111:2385-2399.
- Kobayashi M, Fujiwara K, Takahashi K, et al. Transforming growth factor- $\beta$ -induced secretion of extracellular vesicles from oral cancer cells evokes endothelial barrier instability via endothelial-mesenchymal transition. *Inflamm Regen*. 2022;42:38.
- Fu R, Li Y, Jiang N, et al. Inactivation of endothelial ZEB1 impedes tumor progression and sensitizes tumors to conventional therapies. *J Clin Invest*. 2020;130:1252-1270.
- Hultgren NW, Fang JS, Ziegler ME, et al. Slug regulates the Dll4-notch-VEGFR2 axis to control endothelial cell activation and angiogenesis. *Nat Commun*. 2020;11:5400.
- Welch-Reardon KM, Wu N, Hughes CC. A role for partial endothelial-mesenchymal transitions in angiogenesis? *Arterioscler Thromb Vasc Biol*. 2015;35:303-308.
- Xiao L, Dudley AC. Fine-tuning vascular fate during endothelial-mesenchymal transition. *J Pathol*. 2017;241:25-35.
- Zeisberg EM, Potenta S, Xie L, Zeisberg M, Kalluri R. Discovery of endothelial to mesenchymal transition as a source for carcinoma-associated fibroblasts. *Cancer Res*. 2007;67:10123-10128.
- Cooley BC, Nevado J, Mellad J, et al. TGF- $\beta$  signaling mediates endothelial-to-mesenchymal transition (EndMT) during vein graft remodeling. *Sci Transl Med*. 2014;6:227ra234.
- Pauty J, Usuba R, Takahashi H, et al. A vascular permeability assay using an *in vitro* human microvessel model mimicking the inflammatory condition. *Nanotheranostics*. 2017;1:103-113.



19. Sano T, Nakajima T, Senda KA, et al. Image-based crosstalk analysis of cell-cell interactions during sprouting angiogenesis using blood-vessel-on-a-chip. *Stem Cell Res Ther.* 2022;13:532.
20. Takahashi K, Akatsu Y, Podyma-Inoue KA, et al. Targeting all transforming growth factor- $\beta$  isoforms with an fc chimeric receptor impairs tumor growth and angiogenesis of oral squamous cell cancer. *J Biol Chem.* 2020;295:12559-12572.
21. Kodama S, Podyma-Inoue KA, Uchihashi T, et al. Progression of melanoma is suppressed by targeting all transforming growth factor- $\beta$  isoforms with an fc chimeric receptor. *Oncol Rep.* 2021;46:197.
22. Tokizaki S, Podyma-Inoue KA, Matsumoto T, et al. Inhibition of TGF- $\beta$  signals suppresses tumor formation by regulation of tumor microenvironment networks. *Cancer Sci.* 2023;32(12):e4823. doi:10.1002/pro.4823
23. Abramsson A, Lindblom P, Betsholtz C. Endothelial and non-endothelial sources of PDGF-B regulate pericyte recruitment and influence vascular pattern formation in tumors. *J Clin Invest.* 2003;112:1142-1151.
24. Kokudo T, Suzuki Y, Yoshimatsu Y, Yamazaki T, Watabe T, Miyazono K. Snail is required for TGF $\beta$ -induced endothelial-mesenchymal transition of embryonic stem cell-derived endothelial cells. *J Cell Sci.* 2008;121:3317-3324.
25. Mihira H, Suzuki HI, Akatsu Y, et al. TGF- $\beta$ -induced mesenchymal transition of MS-1 endothelial cells requires Smad-dependent cooperative activation of rho signals and MRTF-A. *J Biochem.* 2012;151:145-156.
26. Akatsu Y, Takahashi N, Yoshimatsu Y, et al. Fibroblast growth factor signals regulate transforming growth factor- $\beta$ -induced endothelial-to-myofibroblast transition of tumor endothelial cells via Elk1. *Mol Oncol.* 2019;13:1706-1724.
27. Okabe K, Kobayashi S, Yamada T, et al. Neurons limit angiogenesis by titrating VEGF in retina. *Cell.* 2014;159:584-596.
28. Watabe T, Nishihara A, Mishima K, et al. TGF- $\beta$  receptor kinase inhibitor enhances growth and integrity of embryonic stem cell-derived endothelial cells. *J Cell Biol.* 2003;163:1303-1311.
29. Yoshimatsu Y, Kimuro S, Pauty J, et al. TGF-beta and TNF-alpha cooperatively induce mesenchymal transition of lymphatic endothelial cells via activation of activin signals. *PLoS One.* 2020;15:e0232356.
30. Cacheux J, Bancaud A, Alcaide D, et al. Endothelial tissue remodeling induced by intraluminal pressure enhances paracellular solute transport. *iScience.* 2023;26:107141.
31. Elgueta R, Benson MJ, de Vries VC, Wasiuk A, Guo Y, Noelle RJ. Molecular mechanism and function of CD40/CD40L engagement in the immune system. *Immunol Rev.* 2009;229:152-172.
32. Greene JA, Portillo JA, Lopez Corcino Y, Subauste CS. CD40-TRAF signaling upregulates CX3CL1 and TNF- $\alpha$  in human aortic endothelial cells but not in retinal endothelial cells. *PLoS One.* 2015;10:e0144133.
33. Lee A, Papangeli I, Park Y, et al. A PPAR $\gamma$ -dependent miR-424/503-CD40 axis regulates inflammation mediated angiogenesis. *Sci Rep.* 2017;7:2528.
34. Luo H, Xia X, Huang LB, et al. Pan-cancer single-cell analysis reveals the heterogeneity and plasticity of cancer-associated fibroblasts in the tumor microenvironment. *Nat Commun.* 2022;13:6619.
35. Trapnell C, Cacchiarelli D, Grimsby J, et al. The dynamics and regulators of cell fate decisions are revealed by pseudotemporal ordering of single cells. *Nat Biotechnol.* 2014;32:381-386.
36. Hellenthal KEM, Brabenec L, Wagner NM. Regulation and dysregulation of endothelial permeability during systemic inflammation. *Cells.* 2022;11:1935.
37. Yang Y, Luo NS, Ying R, et al. Macrophage-derived foam cells impair endothelial barrier function by inducing endothelial-mesenchymal transition via CCL-4. *Int J Mol Med.* 2017;40:558-568.
38. Henn V, Slupsky JR, Gräfe M, et al. CD40 ligand on activated platelets triggers an inflammatory reaction of endothelial cells. *Nature.* 1998;391:591-594.
39. Arciniegas E, Becerra A, de Sanctis JB, Graterol A, Ramírez R. CD40 and CD40L expression in the chicken embryo aorta: possible role in the endothelial-mesenchymal transdifferentiation process. *Anat Rec A Discov Mol Cell Evol Biol.* 2003;274:942-951.
40. Ma J, Sanchez-Duffhues G, Goumans MJ, Ten Dijke P. TGF- $\beta$ -induced endothelial to mesenchymal transition in disease and tissue engineering. *Front Cell Dev Biol.* 2020;8:260.

## SUPPORTING INFORMATION

Additional supporting information can be found online in the Supporting Information section at the end of this article.

**How to cite this article:** Takahashi K, Kobayashi M, Katsumata H, et al. CD40 is expressed in the subsets of endothelial cells undergoing partial endothelial-mesenchymal transition in tumor microenvironment. *Cancer Sci.* 2024;115:490-506. doi:10.1111/cas.16045